

Photochemical Pump and NMR Probe to monitor the formation and fast kinetics of hyperpolarized metal dihydrides

Authors

Barbara Procacci^{ab}, Pedro M. Aguiar^b, Meghan. E. Halse^{ab}, Robin N. Perutz^{b*} and Simon. B. Duckett^{ab*}

Fig. S1. Test to check reproducibility of signal intensity.

Fig. S2. Plot for T_1 measurements of the hydride resonances of an optically diluted solution of **2** in C_6D_6 .

Fig. S3. Plot for the lifetime measurement of the $I_z S_z$ spin state for the hydride resonances of an optically diluted solution of **2** in C_6D_6 .

Fig. S4. Spectra simulated for a two-spin AB system after the application of a 45° pulse.

Fig. S5. Hydride (top: δ -8.5, bottom: δ -14.9) signal integrals of **2** versus τ (time) for a series of $^1H\{^{31}P\}$ NMR spectra recorded at different p - H_2 pressures.

Fig. S6. Plot of pseudo-first-order rate constants k_{obs} for the decay of the transients obtained upon TR-NMR (355 nm) of complex **2** in benzene vs the pressure of quenching gas (H_2) at 315 K.

Fig. S7. Eyring plot for the H_2 addition to **1** photogenerated from **2**.

Fig. S8. Chemical shifts (δ) and coupling constants (J) for complexes **2a*** and **3***.

Fig. S9. Hydride region of the 1H NMR spectrum of a C_6D_6 solution of **2*** with excess PPh_3 .

Fig. S10. Proposed dimeric structures for the major by-products observed under hyperpolarised conditions.

Fig. S11. Hydride region of the 1H NMR spectrum of a C_6D_6 solution of **2** showing the newly formed dimeric species.

Fig. S12. Hydride region of the 1H NMR spectrum of a C_6D_6 solution of a mixture of **2** and **1** exposed to 32 laser shots.

Fig. S13. 2D-COSY run under hyperpolarised conditions showing cross peaks between the newly formed species.

Table S1. k_{obs} determined at different hydrogen pressures by TR-NMR for the hydride at δ -14.9.

Table S2. k_{obs} determined at different hydrogen pressures by transient UV-Vis spectroscopy.

Table S3. k_{obs} and k_2 determined at 4.42 bar of H_2 by photochemical-pump NMR-probe method at different temperatures.

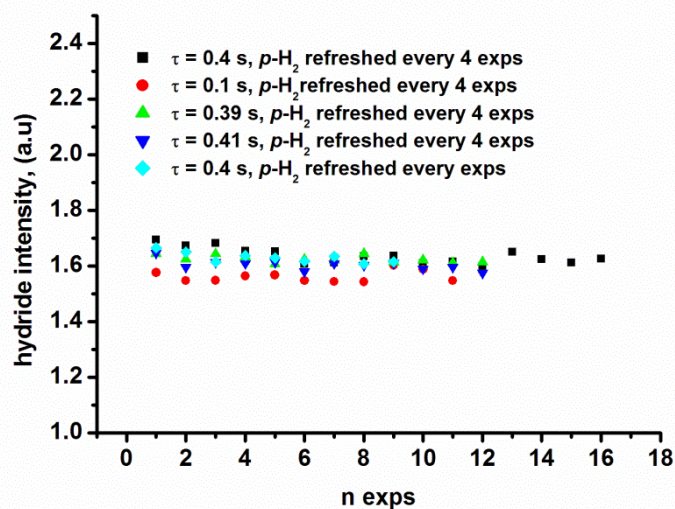


Fig. S1. Test to check reproducibility of signal intensity. The experiments were run at the same τ and shaken every four points ($\tau = 0.4$ s black square, $\tau = 0.1$ s red circle, $\tau = 0.39$ s green triangle, $\tau = 0.41$ s blue triangle) and the last run was done shaking each single point ($\tau = 0.4$ s azure diamond).

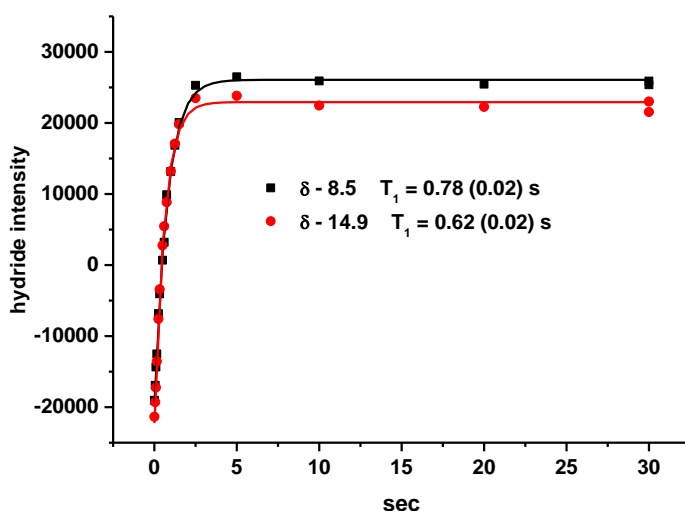


Fig. S2. T_1 inversion recovery measurements for the hydride resonances of an optically dilute solution of **2** in C_6D_6 . Black squares/red circles: experimental points. Black /red lines: lines of best fit to the points by an inversion recovery exponential function.

The thermal T_1 for the hydride resonances of an optically dilute solution of **1** were determined to be 0.78 ± 0.02 s for the hydride resonating at $\delta - 8.5$ and 0.62 ± 0.02 s for the one resonating at $\delta - 14.9$.

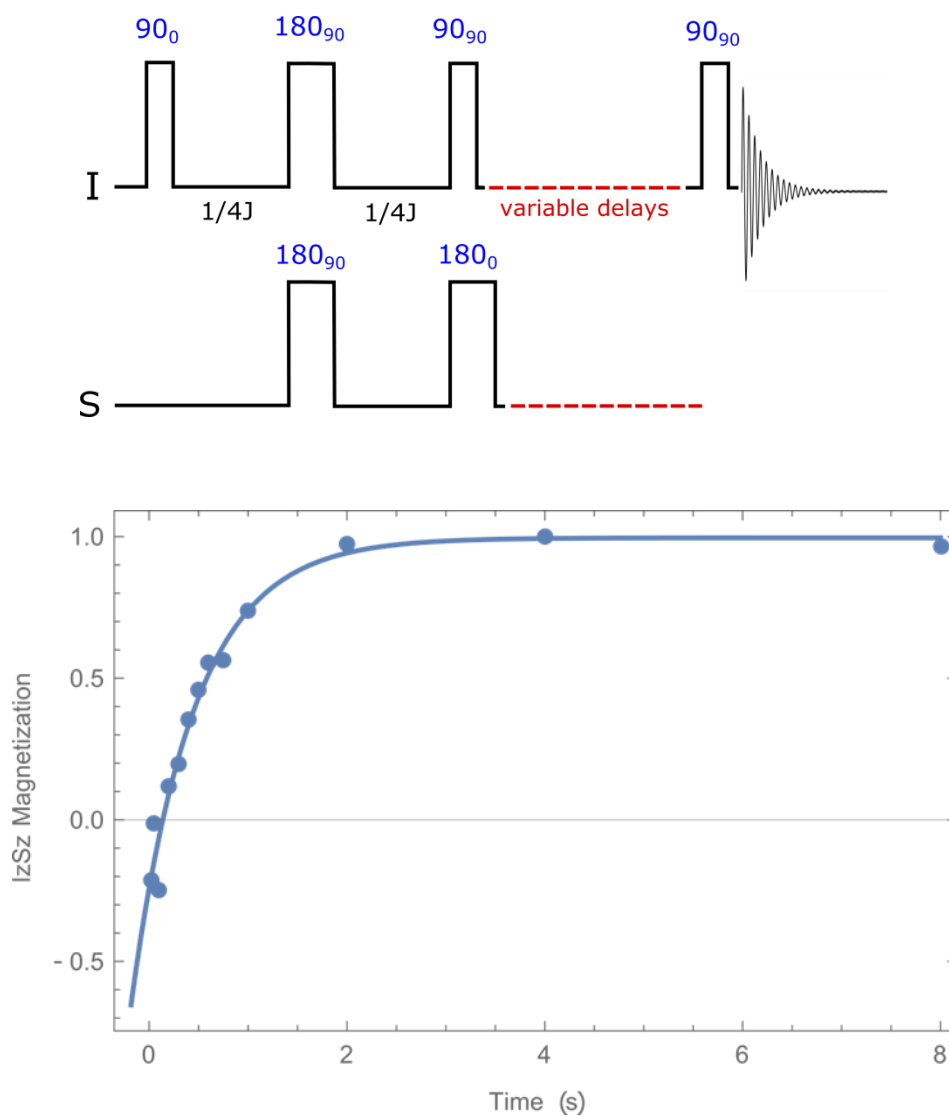


Fig. S3. Lifetime measurements for the $I_z S_z$ spin state of the hydride resonances of an optically dilute solution of **2** in C_6D_6 on a 600 MHz spectrometer. The $I_z S_z$ spin state was created from thermal magnetization by employing pulse sequences (top).^{1,2} A fit to an inversion recovery exponential function yields a lifetime of 0.64 ± 0.08 s (bottom) which compares well with the values suggested by the photochemical pump NMR probe experiments of 0.67 ± 0.11 s.

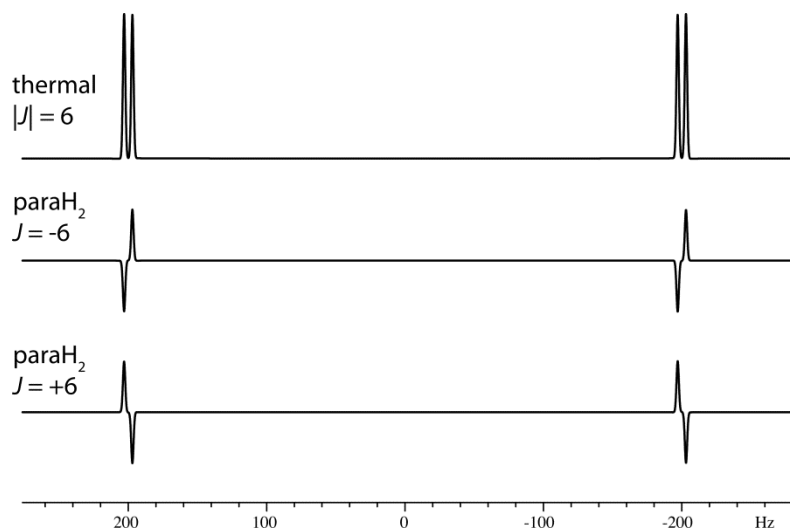
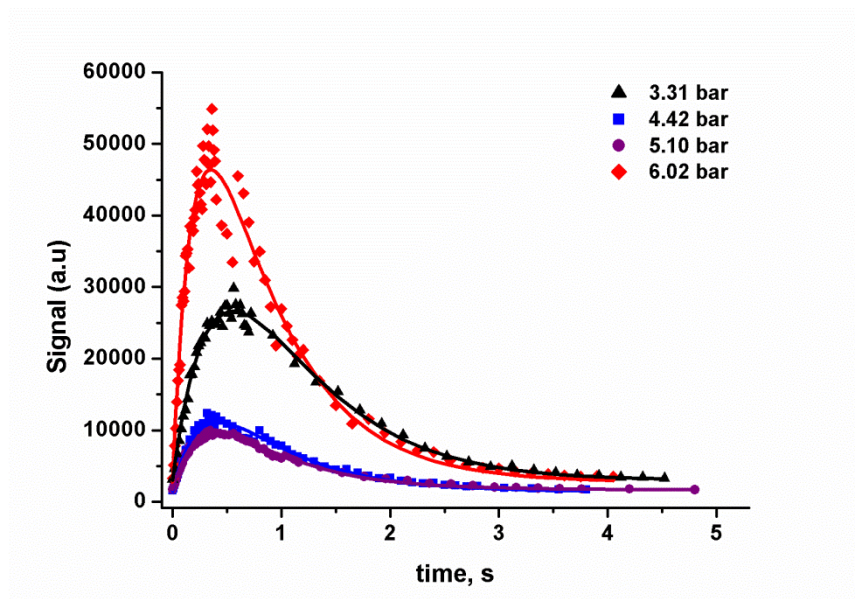
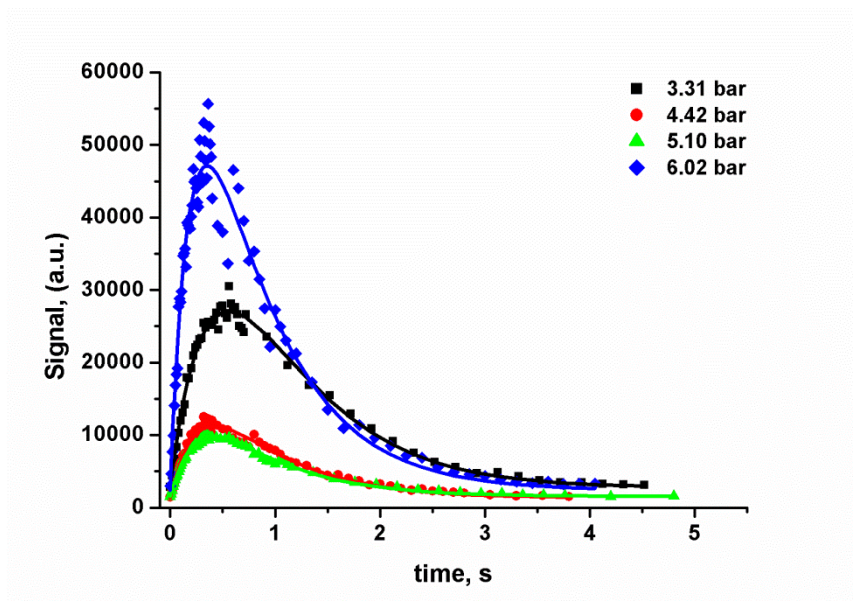


Fig. S4. Spectra simulated³ for a two-spin AB system after the application of a 45° pulse to a thermal system (initial operator: $I_{1z} + I_{2z}$) and *p*-H₂ derived system (initial operator: $-I_{1z}I_{2z}$) with positive and negative J-couplings. Here we assume the standard sign convention for a single C-H bond *J* coupling being positive.⁴





Fig, S5. Hydride (top: δ -8.5, bottom: δ -14.9) signal integrals of **2** versus τ (time) for a series of $^1\text{H}\{^{31}\text{P}\}$ NMR spectra recorded at different $p\text{-H}_2$ pressures. Coloured symbols are experimental points while coloured lines reflect the corresponding fit according to Eq. 2 where R_1 was set to be optimised as a shared parameter in the fit of the entire dataset.

Table S1. k_{obs} determined at different hydrogen pressures by photochemical-pump NMR probe method for the hydride at δ -14.9 at 298 K.

H_2 pressure bar	Hydride at δ -14. $k_{\text{obs}} \text{ s}^{-1}$
3.31	2.2 ± 0.2
4.42	3.6 ± 0.4
5.10	3.8 ± 0.5
6.02	4.9 ± 0.3

Table S2. k_{obs} determined at different hydrogen pressures by transient UV-Vis spectroscopy.

H_2 pressure bar	$k_{\text{obs}}, \text{ s}^{-1}$
1.88	1.84 ± 0.04
2.42	2.06 ± 0.03
3.37	2.60 ± 0.04
4.27	4.06 ± 0.04
4.90	4.31 ± 0.04

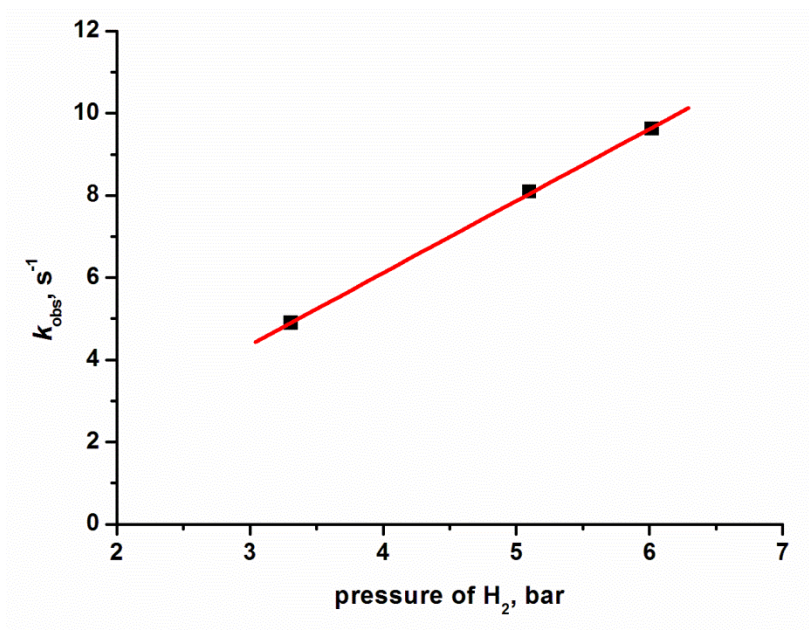


Fig. S6. Plot of pseudo-first-order rate constants k_{obs} (determined by setting R_1 as a shared parameter in the polynomial fitting) for the decay of the transient obtained from photochemical pump - NMR probe (355 nm) of complex **2** in benzene vs the pressure of quenching gas (H_2) at 315 K. The line through the points shows the best fit.

Table S3. k_{obs} and k_2 determined at 4.42 bar of H_2 by photochemical-pump NMR-probe method at different temperatures.

T, K	k_{obs}, s^{-1}	$k_2, s^{-1} M^{-1}$
283	1.82 ± 0.04	142 ± 3
295	4.1 ± 0.4	317 ± 31
315	12.9 ± 1.7	$(1.01 \pm 0.14) \times 10^3$

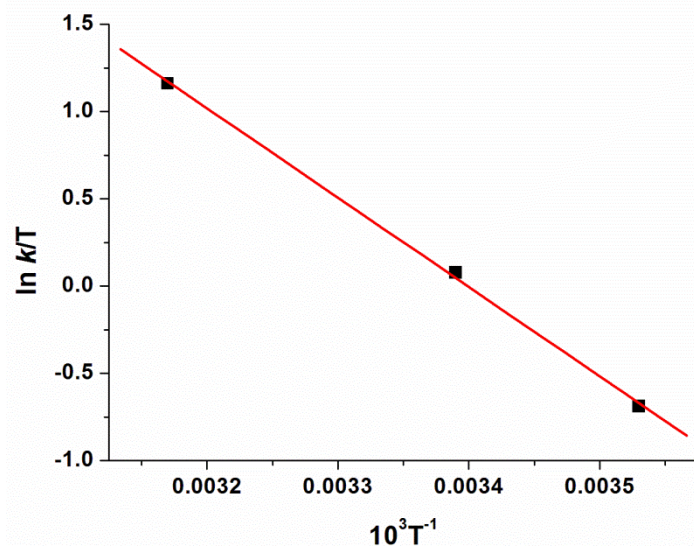


Fig. S7. Eyring plot for the H₂ addition to **1** photogenerated from **2** under 4.42 bar of H₂; $k = k_2 = k_{\text{obs}} / ([\text{H}_2] \times \text{solubility of H}_2)$; we assume a constant concentration of *p*-H₂ in a closed vessel over this temperature range.



δ -9.2 *trans* to CO (ddd) $^2J_{\text{PH}}$ 20, 14 Hz, $^2J_{\text{HH}}$ -5 Hz, **2a***

δ -11.5 *trans* to P (ddd) $^2J_{\text{PH}}$ 126, 26 Hz, $^2J_{\text{HH}}$ -5 Hz, **2a***

δ -11.2 *trans* to P (dtd) $^2J_{\text{PH}}$ 144, 19 Hz, $^2J_{\text{HH}}$ -4 Hz, **3***

δ -17.6 *trans* to I (dtd, but apparent dq) $^2J_{\text{PH}}$ 20, 14 Hz, $^2J_{\text{HH}}$ -4 Hz, **3***

Fig. S8. Chemical shifts (δ) and coupling constants (J) for complexes **2a*** and **3*** measured from the hydride resonances under hyperpolarised conditions. The $^2J_{\text{HH}}$ values are estimates measured from the anti-phase peak separations. Simulations in previous work showed that precise HH couplings are not easily obtained from such anti-phase peaks because of internal cancellation due to the linewidths of the overlapping components.

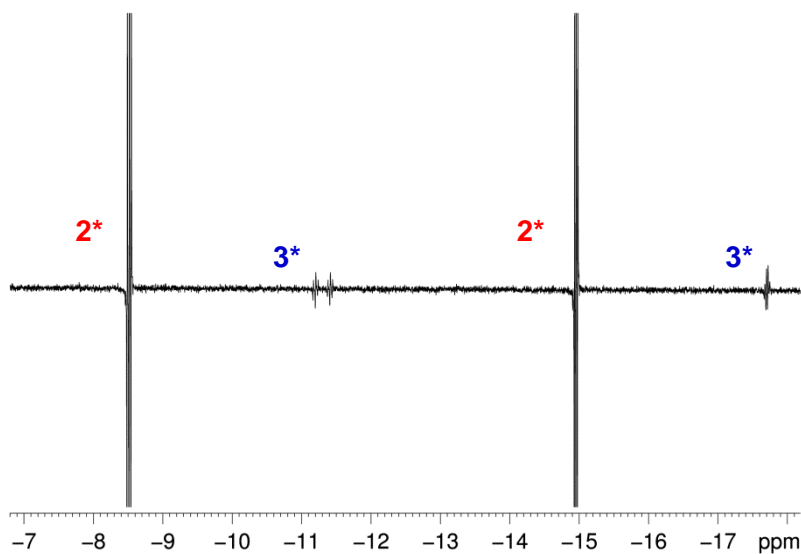
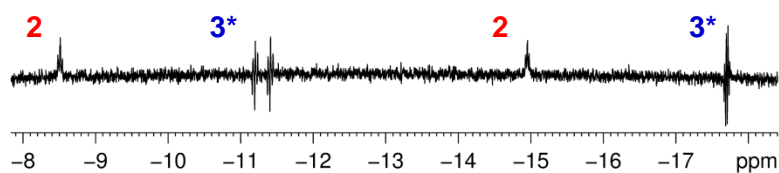


Fig. S9. Top: Hydride region of the ^1H NMR spectrum of a C_6D_6 solution of **2** under $p\text{-H}_2$ with excess PPh_3 showing the formation of **3*** at room temperature. Bottom: Hydride region of the ^1H NMR spectrum of a C_6D_6 solution of **2** with excess PPh_3 after 32 laser shots. The major species is **2*** and the minor by-product is **3***. The formation of **2a***, previously observed, was suppressed in this case by excess PPh_3 in solution.

Dimeric Species

In addition to hyperpolarized hydride signals of **2**, new enhanced hydride signals in the region δ -18 to -22 (Fig. S10) were detected when the temperature of an optically dilute solution of **2** under $p\text{-H}_2$ was raised to 335 K (Fig. S11). These dimeric species remained visible by PHIP for several minutes. These signals could also be accessed after multiple laser shots at lower temperatures (> 16 laser shots at 315 K).

Two of the extra resonances (δ -18.6 and δ -21.2) could also be made stronger if a mixture of **2** and its 16-electron precursor $\text{Ir}(\text{CO})(\text{PPh}_3)_2$ **1** were dissolved in C_6D_6 solution and exposed to $p\text{-H}_2$ atmosphere under both thermal and photochemical conditions (Fig. S12). The enhanced hydride resonances were found to exhibit a 1:1 intensity ratio and proved to be correlated by 2D-COSY (Fig S13). Furthermore, their antiphase signals simplified into doublets under ^{31}P decoupling. The hydrides also couple to two sets of inequivalent phosphorus nuclei such that they exhibit $^2J_{\text{PH}}$ couplings of 16

and 19 Hz respectively while sharing a $^2J_{\text{HH}}$ splitting of -6 Hz. The ^{31}P signal responsible for the triplet splitting was located at δ 19.6 and 22.9 in a 2D HMQC measurement.

A more concentrated solution of the mixture was photolysed overnight under steady state conditions ($\lambda > 345$ nm, room T); although the main product observed by ^1H NMR spectroscopy was still **1**, LIFDI mass spectrometry revealed a m/z peak of 1217.36 which corresponds to the mass of $[\text{Ir}(\text{CO})(\text{PPh}_3)_2]$.

We can therefore speculate that the by-products formed in our experiments are dimers which are observed only under hyperpolarized conditions and are capable of reacting with H_2 on a faster timescale than **2**. This supports what is reported in the literature by time-resolved studies.^{6,7} Their formation appears to be strongly dependent on the concentration of both **2** and **1**, but more importantly they are not detected when working with the optically dilute solution of **2** with a single laser shot and therefore do not interfere with our measurements. Having ensured that the reactivity of these dimeric species does not interfere with our pump-probe measurements, we consider further experiments into the characterization of these species to be beyond the scope of this paper.

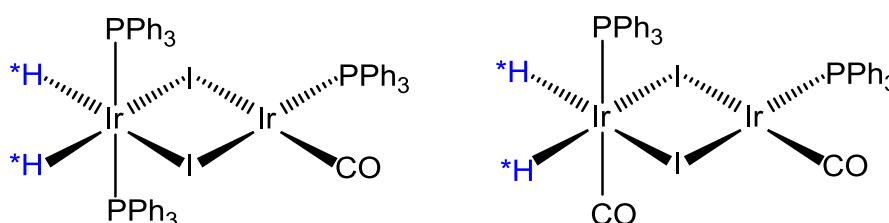


Fig. S10. Proposed dimeric structures for the major by-products observed under hyperpolarised conditions.

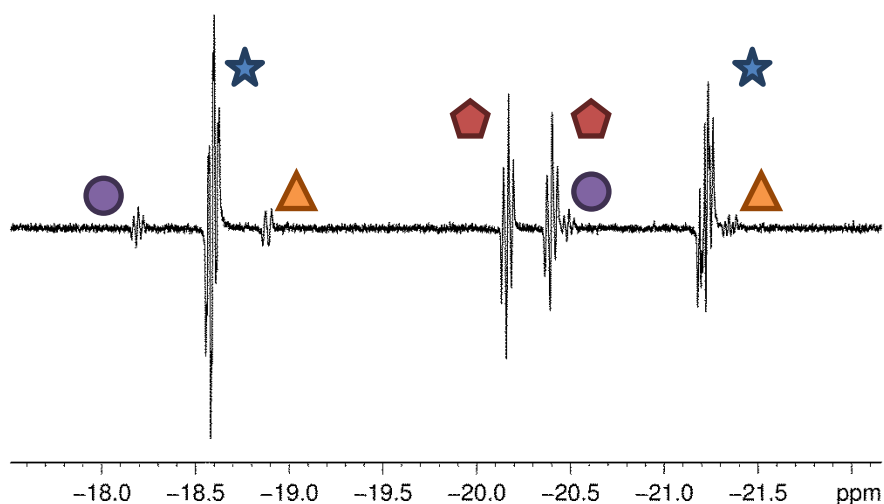


Fig. S11. High field hydride region of the ^1H NMR spectrum of a C_6D_6 solution of **2** showing the newly formed dimeric species detected only under hyperpolarised conditions at 335 K.

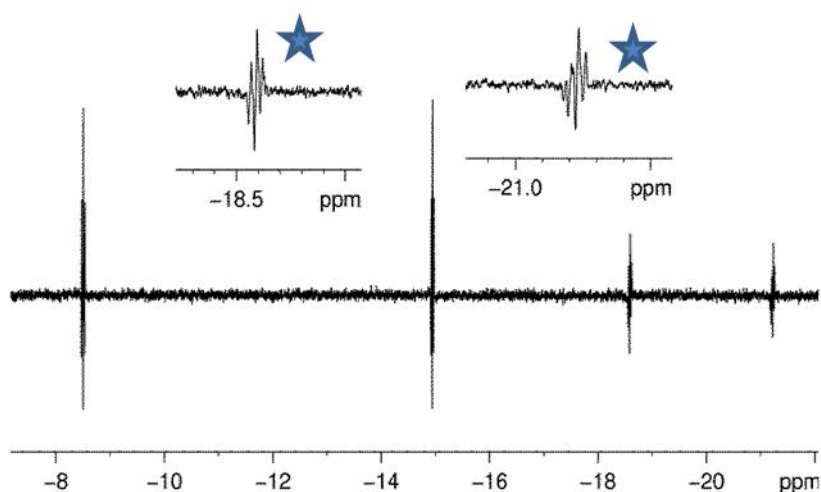


Fig. S12. Hydride region of the ^1H NMR spectrum of a C_6D_6 solution of a mixture of **2** and **1** exposed to 32 laser shots. The major peaks belong to **2***, the minor species is assigned to one of the dimeric species formed. Inset: Expansion of the hydride resonances of the dimeric species.

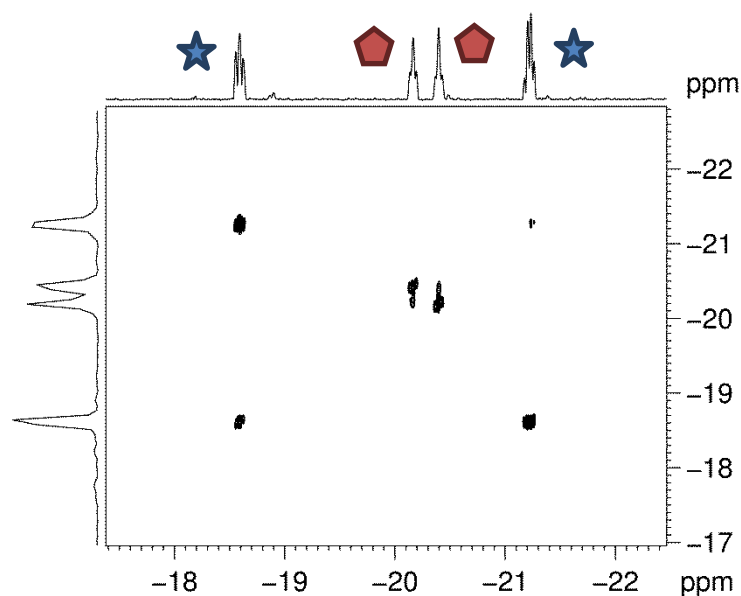


Fig. S13. ^1H - ^1H 2D-COSY NMR spectrum run under hyperpolarised conditions showing cross peaks between the newly formed species. The observation of the cross peak was possible because the enhancement on these compounds lasts for a few minutes and therefore signal averaging was possible. This 2D-COSY spectrum was acquired using a $\pi/4$ - t_1 - $\pi/4$ - t_2 pulse sequence.⁵

References:

1. D. Canet, *Prog. Nucl. Magn. Reson. Spectrosc.*, 1989, **21**, 237-291.
2. G. Jaccard, S. Wimperis, G. Bodenhausen, *Chem. Phys. Lett.*, 1987, **138**, 601.
3. M. Bak, J. T. Rasmussen, N. C. Nielsen, *J Magn. Reson.*, 2000, **147**, 296-330.
4. C. J. Jameson in *Multinuclear NMR*, ed. J. Mason, Plenum Press, New York, 1987, 89-131.
5. C. J. Sleigh, S. B. Duckett and B. A. Messerle *J. Chem. Soc. Chem. Comm.*, 1996, 2395-2396.
6. D. A. Wink and P. C. Ford, *J. Am. Chem. Soc.*, 1985, **107**, 5566-5567.
7. R. H. Schultz, *J. Organomet. Chem.*, 2003, **688**, 1-4.